Energy Equip. Sys./ Vol. 12/No. 4/December 2024/ 327-340

ENERGY EQUIPSYS

Energy Equipment and Systems

www.energyequipsys.com

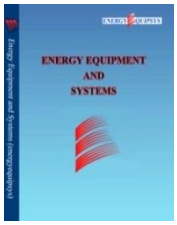

Experimental assessment of a solar dryer enhanced by a porous absorber plate and PCM heat storage

Manuscript Type
Research Paper

Authors

Hussein Khalaf Jobair[a]*
Mohammed Nima[b]

[a] Energy Engineering Department, College of Engineering, University of Baghdad, Baghdad, Iraq

[b] Mechanical Engineering Department, College of Engineering, University of Baghdad, Baghdad, Iraq

Article history:
Received : 15 February 2024
Revised : 10 March 2024
Accepted : 11 March 2024

ABSTRACT

This research presents an experimental investigation into a double-pass counter-flow solar air heater (DCSAH) incorporating a copper foam absorber plate and PCM heat storage for drying purposes, conducted with a no-load case under Iraq's meteorological conditions in Baghdad (Latitude 33.3^{0}N). A total of 36 kilograms of paraffin wax serves as the phase change material, divided equally into two portions and enclosed within separate heat exchangers. The investigation examines the effects of mass flow rate, PCM utilization, and incident solar radiation on various parameters, including outlet air temperature, heat gained, thermal efficiency, benefit factor, and pressure drop across the solar collector. A comparative analysis is performed with a flat plate solar dryer featuring a traditional absorber plate. The findings reveal that, compared to a flat absorber plate, the DCSAH's thermal efficiency improves by (15%, 19%, and 22%) for air mass flow rates of 0.0076, 0.0118, and 0.0136 kg/s, respectively, when equipped with a copper foam absorber plate without PCM. Furthermore, the benefit factor surpasses 1 for an air mass flow rate of 0.0118 kg/s. Comparative analysis with previous studies indicates good agreement between the findings of this study and prior works.

Keywords: Solar Dryer, PCM, Copper Foam, Thermal Efficiency, Benefit Factor.

1. Introduction

For centuries, the drying process has served as a method for preserving a variety of food and agricultural products. By reducing the natural moisture levels inherent to these products, drying effectively inhibits the growth of microbial organisms and enzymatic agents, thus preventing product deterioration. Typically, hot air is circulated over the products during the drying process, facilitating moisture evaporation and reducing water content. Different energy sources can be employed to supply the essential thermal energy needed for the desiccation process. Conventional approaches typically entail the combustion of fuels like LPG, coal, or biomass to produce hot air for drying [1]. Nevertheless, in recent times, there has been a growing emphasis on harnessing sustainable energy sources, notably solar energy, for drying applications.

Solar drying involves capturing the thermal energy emitted by sunlight to facilitate the drying of agricultural products. This method offers numerous advantages, including

* Corresponding author: Hussein Khalaf Jobair
Energy Engineering Department, College of Engineering, University of Baghdad, Baghdad, Iraq.
E-mail address: hussein.khalf@coeng.uobaghdad.edu.iq

sustainability, cost-effectiveness, and environmental friendliness [2]. Statistics indicate that agricultural product losses in developing countries typically range between 30% and 40% of total production due to inadequate treatment, transportation, and storage facilities [3]. The implementation of suitable solar drying systems has the potential to substantially decrease post-harvest losses of agricultural commodities in rural areas of developing countries [4].

The effectiveness of the solar drying system significantly depends on the performance of the solar air collector (SAH). The compact design of SAH allows for easy construction using affordable materials. Offering user-friendly operation, it efficiently harnesses abundant solar energy to produce hot air, rendering it suitable for a wide range of industrial and drying purposes. However, the thermal efficiency of SAHs is restricted by the absorber plate's relatively poor heat transfer coefficient to the working fluid. Consequently, numerous investigations have been conducted to improve the operational efficiency of SAHs, particularly for drying purposes.

Various design approaches have been investigated to enhance the SAH absorber plate-operational fluid convective heat transfer coefficient. These approaches include using a corrugated absorber plate [5-8], attaching fins above and below the absorber plate in different shapes and arrangements [9-11], incorporating corrugated fins [12,13], introducing roughness geometry [14], and employing a porous absorber plate [15-16]. Furthermore, integrating SAHs with thermal energy storage mechanisms can enhance their thermal performance [17-21].

Alkilani et al. [22] investigated the application of a single glass cover solar collector augmented with phase change material (PCM) for drying purposes. The PCM was positioned between the glazing sheet and the absorber plate in a row of cylinders. Simulations were carried out with the initial air temperature set at 28ºC and the PCM starting as a liquid at 50ºC. The study investigated the effects of airflow, output temperature, and PCM freezing time. The results revealed that higher mass flow rates led to reduced air temperature and prolonged discharge times.

Ramirez et al. [23] formulated a thermodynamic model to evaluate a solar dryer (ISD) equipped with PCM as a thermal storage. Their study involved comparing this model with empirical real-world data. The ISD configuration incorporated PCM in one of two identical dryers, operating in daytime and nighttime modes. The model encompassed dimensions, properties of components (such as glass cover, absorber plate, PCM), and established energy balances with boundary conditions. It predicted temperatures, heat efficiencies, and difficult-to-measure variables like liquid fraction and heat losses. The findings demonstrated that PCM enhanced the nighttime performance and operational duration of the ISD.

In a study executed by El Khadraoui et al. [24], an indirect solar dryer equipped with PCM was built and tested. The study delved into the viability of employing a solar air heater integrated with PCM for diurnal energy accumulation and subsequent nocturnal discharge. Moreover, the study examined the charging and discharging dynamics of the PCM compartment, revealing a daily energy efficiency of 33.9% and a daily exergy efficiency of 8.5%. Findings demonstrated that the solar energy reservoir elevated the temperature within the drying chamber by 4-16°C above ambient levels throughout nocturnal periods, while concurrently diminishing relative humidity by 17-34.5% compared to the solar dryer lacking PCM integration.

To date, no investigations have been conducted on the utilization of open-cell metal foam as an absorber plate in solar drying applications. Open-cell metal foams possess unique attributes, including remarkably high porosity reaching up to 97.5%, high effective thermal conductivity, and a substantial surface-area-to-volume ratio spanning from 1000 to 3000 m^2/m^3, significantly enhancing convective heat transfer due to tortuous flow paths. Additionally, they are lightweight, offer minimal resistance to fluid flow, leading to reduced pressure drop, and exhibit various other favorable mechanical properties [25]. These distinctive characteristics inherent in open-cell metal foams make them a promising candidate for a variety of practical and engineering

implementations. The aims of the current investigation can be outlined as bullet items;

a. Design and fabricate two identical double-pass SAHs for drying purposes under Iraq's meteorological conditions, operating under a no-load scenario.
b. Employing two types of metal foams as absorber plates, namely 10 PPI and 40 PPI.
c. Evaluating the thermal efficiency of the double-pass SAH featuring a metal foam absorber in contrast to the flat absorber.
d. Conducting experimental research on the implementation of PCM for thermal storage and assessing its influence on the thermal efficiency of the constructed system.
e. An experimental investigation examining how air flow rate and sun irradiation affect the solar dryer's thermal performance.

Nomenclature

A_c	Cross-sectional area [m^2]
C_p	Specific heat capacity at constant pressure[J kg^{-1} K^{-1}]
D	Pipe diameter [m]
d	Orifice diameter [m]
h	Water coloumn height [m]
I	Solar irradiation [W/m^2]
m	Mass of air [kg]
$\dot{m}$	Air mass flowrate [kg/s]
p	Static pressure [N/m^2]
Q	Heat transfer [W]
Q_i	Absorbed energy [W]
Q_{pump}	Air pumping power [W]
Q_u	Useful heat gain [W]
R	Specific gas constant [J kg^{-1} K^{-1}]
T	Temperature [K]
V	Air Volume [m^3]

Abbreviation

BF	benefit factor
DCSAH	double-pass counter-flow solar air heater
GI	galvanized Iron
LPG	Liquefied petroleum gas
PCM	Phase change material
PPI	pores per inch
SAH	solar air heater

2. Experimental equipment

Two double-pass SAHs are developed, constructed, and assembled to be identical in design, fabrication, dimensions, and operational conditions, except for the absorber plate type. Each SAH consists of a rectangular wooden box as its main structure, topped with a 4 mm window glass glazing sheet. Positioned within the box are the absorber plate and base plate, the latter constructed from a 1 mm GI sheet placed over a 50 mm polystyrene insulation sheet. In this study, two absorber plates are employed: a 10 PPI copper foam absorber (2000 × 1000 × 10 mm) and a conventional copper absorber (2000 × 1000 × 1 mm). Both upper and lower channels have an identical vertical dimension of 50 mm in height, and the solar collector's trailing edge has an air gap of 20 mm. The airflow follows a specific path: entering through a divergent duct, passing through the upper channel between the glass sheet and absorber, and ultimately moving through the lower channel between the absorber and base plates. The air exits the solar collector through a convergent duct, while the SAH-optimized for the proposed location is slanted at a 33º angle [26]. Each of the two heat exchangers contains 18 kg of paraffin wax as a PCM for the solar dryer systems. Table 1 provides a complete overview of the paraffin wax's thermophysical characteristics. The drying chamber dimensions are 1000 × 760 × 760 mm. Figure 1(a) and 1(b) depict the schematic of the DCSAH and a photograph of the system, respectively. The study was conducted in June 2023. Figure 2 illustrates the solar radiation and ambient temperature recorded on the days of investigation, obtained from the Ministry of Science and Technology / Renewable Energy Department, Baghdad city.

3. Analysis of experimental data

The thermal efficiency of the DCSAH can be defined as the ratio between the solar collector's heat acquired and solar energy assimilated by the absorber plate.

$$\eta_{th} = Q_u/Q_i \quad (1)$$

where;

$$Q_u = \dot{m}C_p(T_{out} - T_{in}) \quad (2)$$

$$Q_i = IA_c \quad (3)$$

Table 1. Thermophysical characteristics of PCM

Property	Value
Density	$900-910[\,\mathrm{kg/m^3}\,](\mathrm{solid})$ $880-890[\,\mathrm{kg/m^3}\,](\mathrm{liquid})$
Melting Temperature	52 ~ 54℃
Latent Heat of Fusion	$160-230[\mathrm{kJ/kg}]$
Thermal Conductivity	$0.34-0.4\ \mathrm{W}m^{-1}{}^{\circ}C^{-1}$
Specific Heat	$3-5\ \mathrm{kJ\ kg}^{-1}{}^{\circ}C^{-1}$
Viscosity	$3.325[\,\mathrm{mm^2/s}\,]$

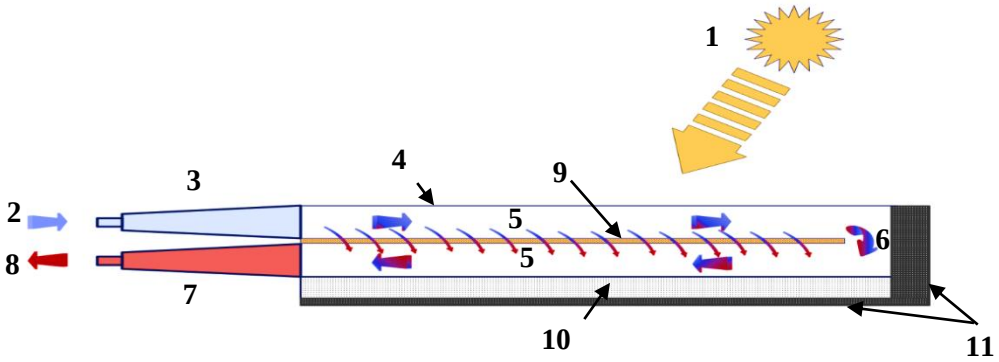

(a): 1. The Sun, 2. Air Inlet, 3. Conical Inlet Section, 4. Single Glass Cover, 5. Air Channel, 6. Air Gap, 7. Conical Outlet Section, 8. Air Outlet

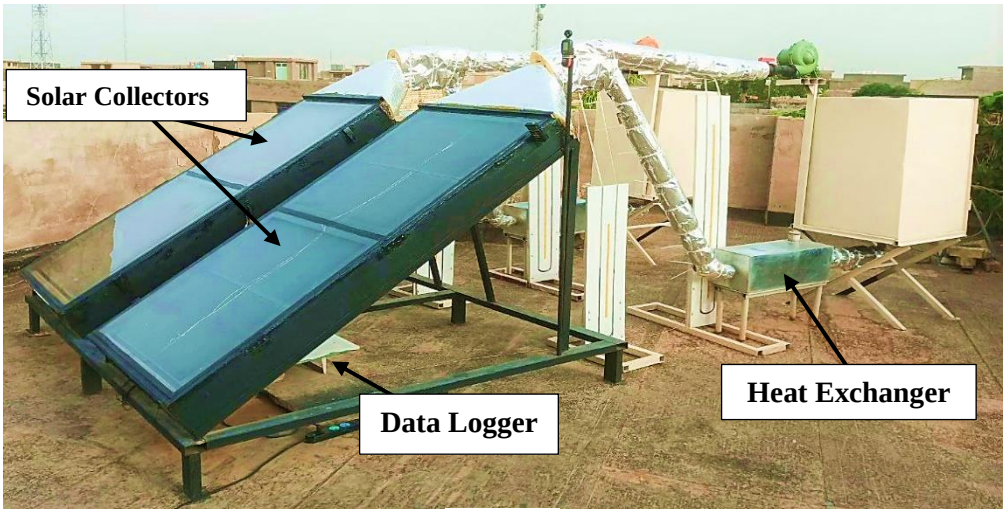

(b)

Fig. 1. (a) A schematic diagram of DCSAH, (b) a photograph of the constructed system, Baghdad, Iraq

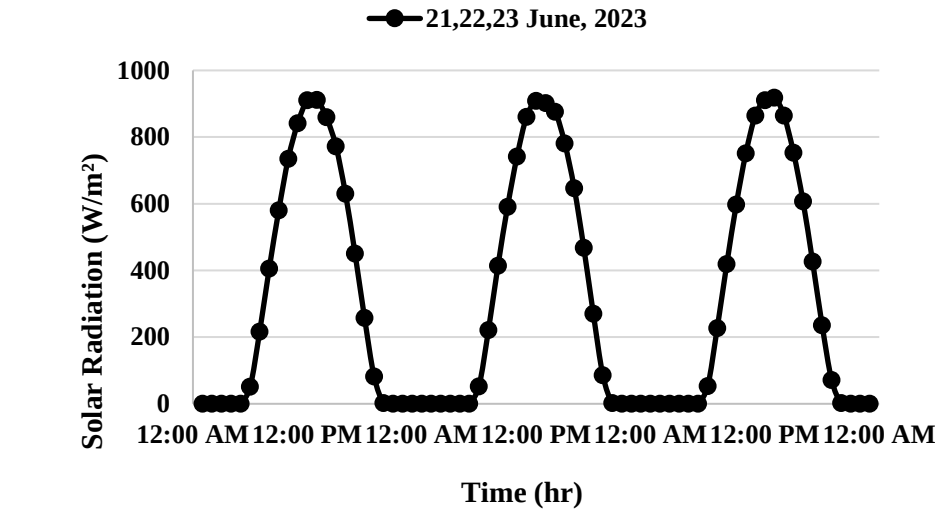

(a)

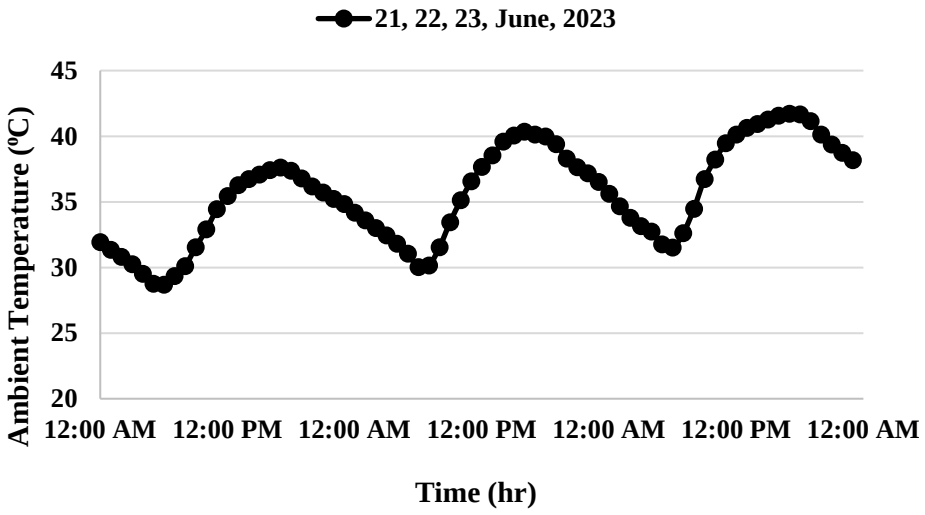

(b)

Fig. 2. (a) Solar radiation vs. time, (b) ambient temperature vs. time

The solar collector inlet temperature, denoted as T_{in}, surpasses the ambient temperature. This temperature elevation is a result of the required pumping power that propels the air toward the solar collector. Equations (4) and (5) describe how this process raises the DCSAH's inlet air temperature.

$$PV = mRT \tag{4}$$

$$Q_{pump} = Q \times P \tag{5}$$

where $A_c = 2.05\ m^2$. ṁ can be calculated using the equation below [27]:

$$\dot{m} = C_d A_o \sqrt{2\rho\Delta p/(1-\beta^4)} \tag{6}$$

where C_d symbolizes the coefficient of discharge, Δp symbolizes the pressure drop across the manometer attached to the orifice meter, A_0 symbolizes the area of the orifice plate's hole, whereas β symbolizes the ratio between the orifice and pipe diameters, $(\beta = d/D)$. The value of the coefficient of discharge is taken as $C_d = 0.62$, and Δp can be calculated from the following relation:

$$\Delta p = \gamma h \tag{7}$$

where γ represents the specific weight (9810 N/m^3 for water).

The assessment of the solar collector's

thermal performance relies on determining both the thermal efficiency and the benefit factor. The benefit factor exemplifies the ratio of heat transfer enhancement achieved by utilizing a porous absorber compared to a conventional absorber, to the increase in pressure drop resulting from employing a porous absorber instead of a conventional one. Equation (8) can be used to determine the benefit factor. [28]:

$$BF = (Q_{u,por}/Q_{u,flat})/(\Delta P_{por}/\Delta P_{flat}) \quad (8)$$

where $Q_{u,por}$, $Q_{u,flat}$ denote the heat gains of the DCSAH with porous and flat absorbers, respectively. ΔP_{por}, ΔP_{flat} denote the pressure drops across the DCSAH with porous and flat absorbers, respectively.

4. Results and Discussion

Figures 3 and 4 depict a time-dependent analysis of air temperature difference in the DCSAH utilizing PCM as a thermal storage. The study investigates both 10 PPI and flat absorber plates across various flow rates. The results manifest that the air temperature difference increases with escalating incident solar radiation, reaching its peak between 12:00 PM and 2:00 PM. A notable observation is that the solar collector lacking PCM exhibits higher air temperature differences during the charging process than the one with PCM, attributed to thermal storage presence. The charging duration for both solar collectors spans from 9:00 AM until approximately 2:00 to 3:00 PM. At 2:00 PM, the solar collector

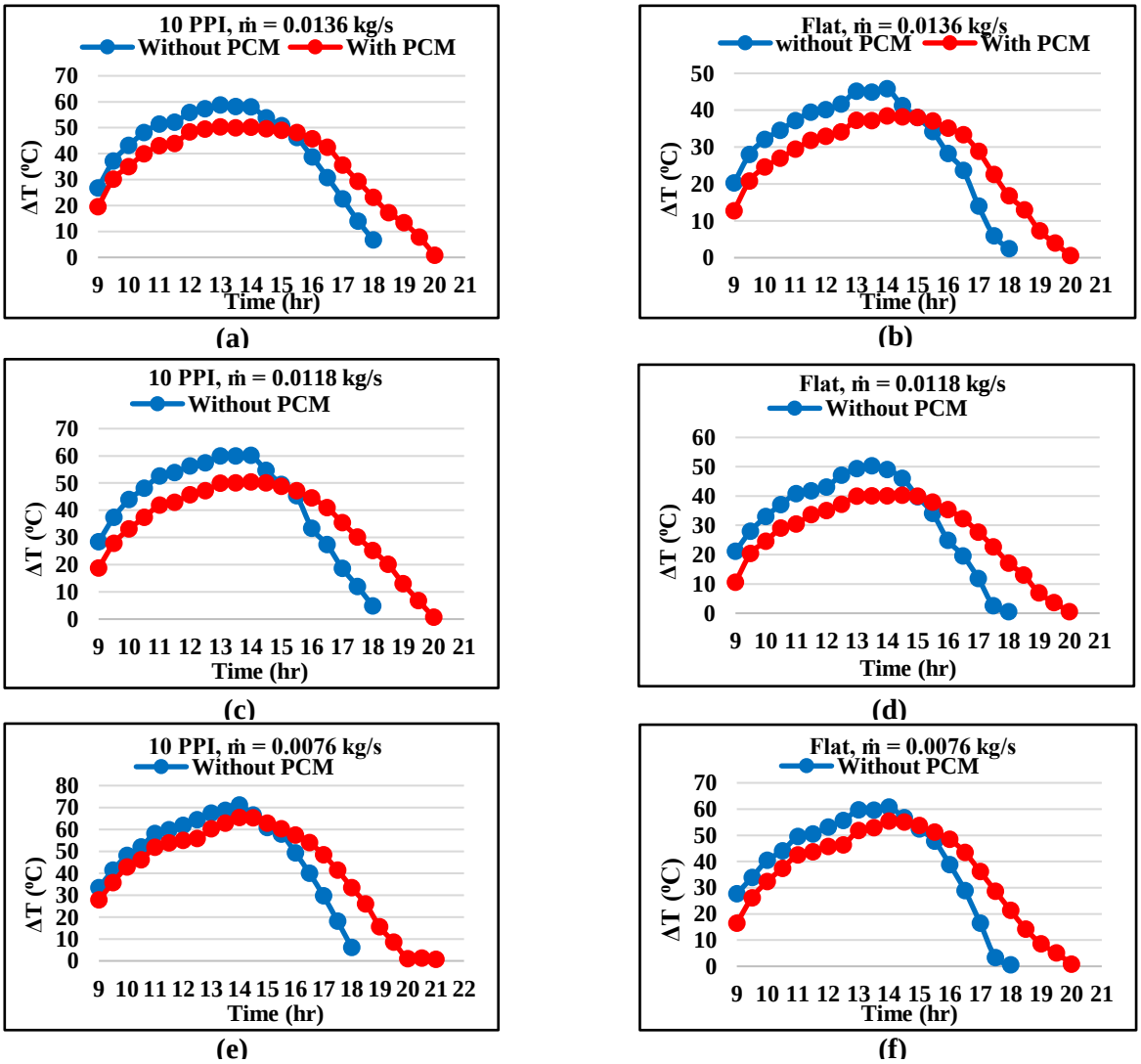

Fig. 3. PCM influence on the time-dependent temperature difference of DCSAH with flat and 10 PPI absorber plates

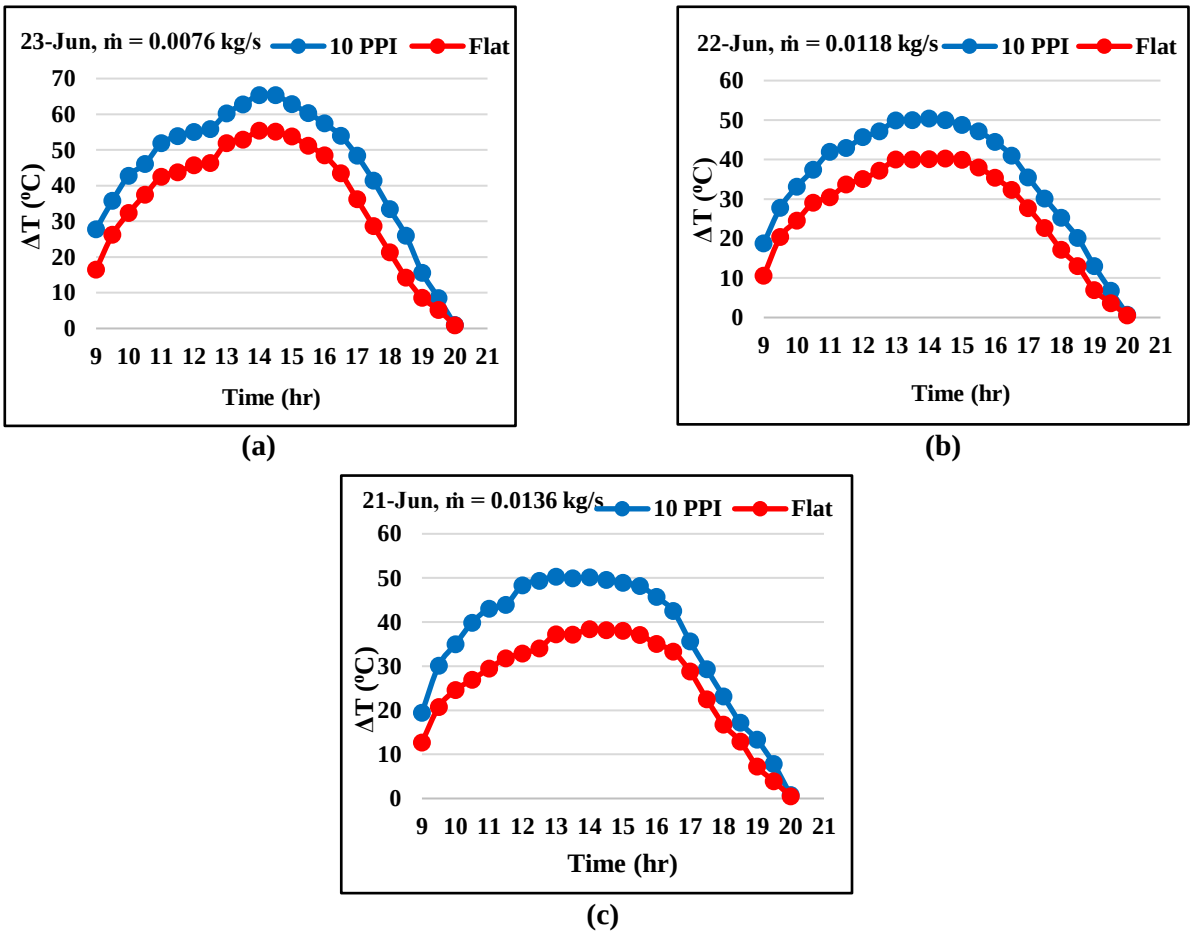

Fig. 4. Comparison between the temperature difference of DCSAH provided with flat and 10 PPI absorber plate

equipped with a porous absorber plate demonstrates maximum air temperature differences of 71.1°C, 60.2°C, and 58.1°C for ṁ = 0.0076, 0.0118, and 0.0136 kg/s, respectively, without employing PCM, and 65.4°C, 50.4°C, and 50°C, respectively, with PCM. Contrarily, for the DCSAH featuring a flat absorber, the study reveals maximum air temperature differences of 60.8°C, 49°C, and 45.8°C, respectively, at ṁ = 0.0076, 0.0118, and 0.0136 kg/s, without utilizing PCM. Conversely, with PCM usage, the maximum air temperature differences decrease to 55.4°C, 40.1°C, and 38.4°C for the same corresponding ṁ. After 2:00 to 3:00 PM, the air temperature difference gradually diminishes, but during the discharge process after 3:00 PM, the DCSAH with PCM exhibits a higher air temperature difference than the configuration lacking PCM, attributed to the release of the storage heat in PCM. Notably, after sunset, the DCSAH's outlet air temperature is 1 to 9 °C higher than the ambient temperature for two hours.

Figures 5 and 6 illustrate the DCSAH's time-dependent heat transfer rate featuring 10 PPI and flat absorber plates, both utilizing PCM for thermal storage. The findings indicate that as incident solar radiation escalates, heat transfer rate for both types of DCSAHs increases, peaking between 1:00 PM and 2:00 PM. After this period, the heat transfer rate gradually declines as incident solar radiation diminishes. Additionally, it has been observed that the rate of heat transfer of DCSAHs utilizing PCM during the charging process is lower compared to those without PCM. Conversely, during the discharge process, solar collectors employing PCM exhibit a greater rate of heat transfer in comparison to those without PCM, attributed to the presence of PCM. Furthermore, the findings reveal that at ṁ = 0.0076, 0.0118, and 0.0136 kg/s, the highest heat transfer rates for a DCSAH featuring a 10 PPI absorber plate and PCM heat storage are 500.3 W, 598.5 W, and 686.3 W, respectively. In contrast, for a DCSAH

featuring a flat absorber and PCM, the corresponding heat transfer rates are 423.7 W, 475.8 W, and 525.8 W for the same flow rates, respectively.

Figure 7 depicts the variation of the time-dependent benefit factor concerning the air mass flow rate, considering $\dot{m}_1$ = 0.0136 kg/s, $\dot{m}_2$ = 0.0118 kg/s, and $\dot{m}_3$ = 0.0076 kg/s. The benefit factor drops below unity at the maximum flow rate attributed to the higher Δt experienced by the ṁ when utilizing a 10 PPI absorber plate. Consequently, despite the high rate of heat transfer achieved by the DCSAH featuring the porous absorber, the new DCSAH's thermal performance is deemed unfeasible at ṁ. Conversely, at ṁ = 0.0118 kg/s, the benefit factor exceeds 1, indicating superior thermal performance contrasted to the other ṁ values.

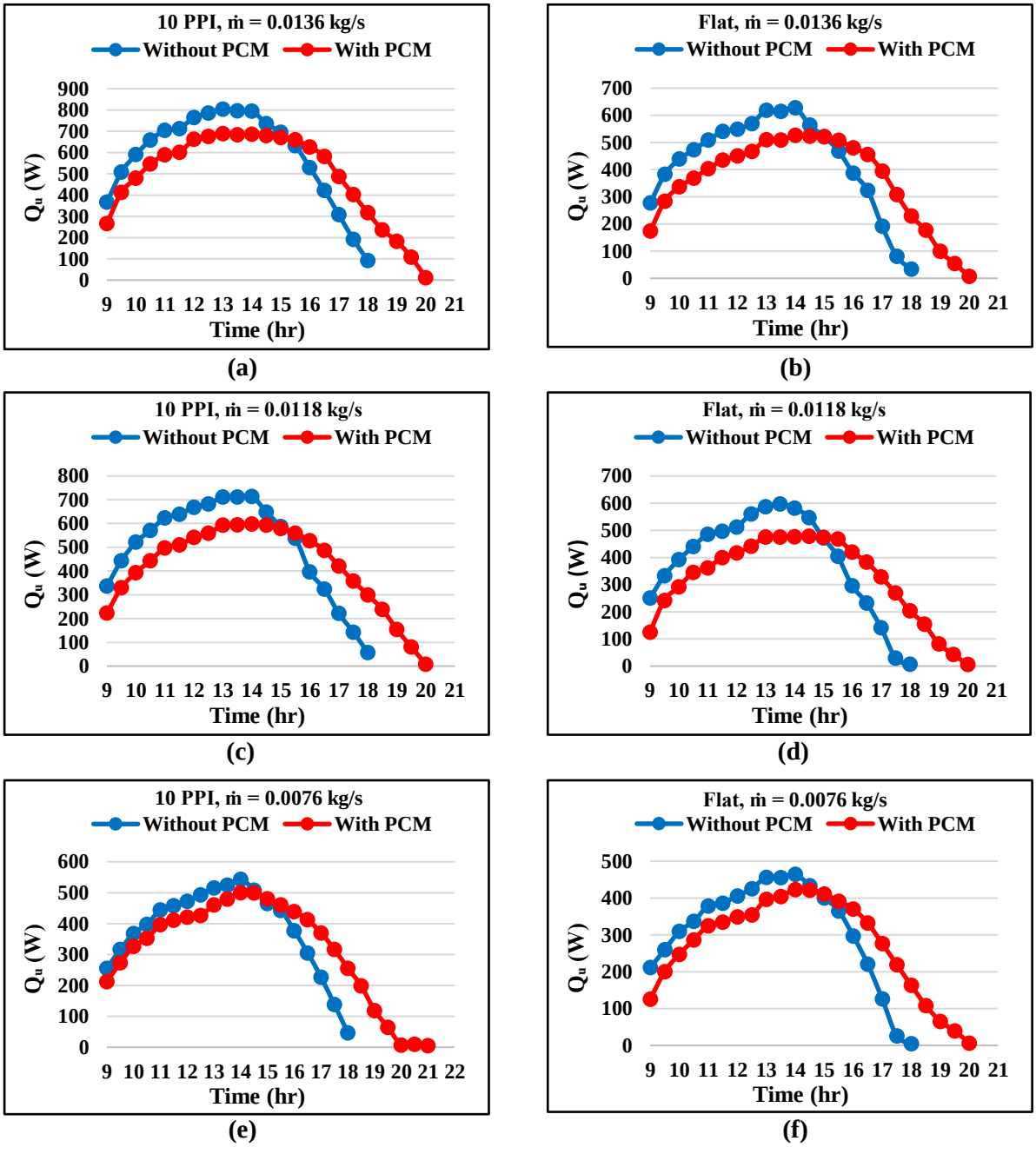

Fig. 5. PCM influence on the heat transfer rate of DCSAH provided with flat and 10 PPI absorber plates

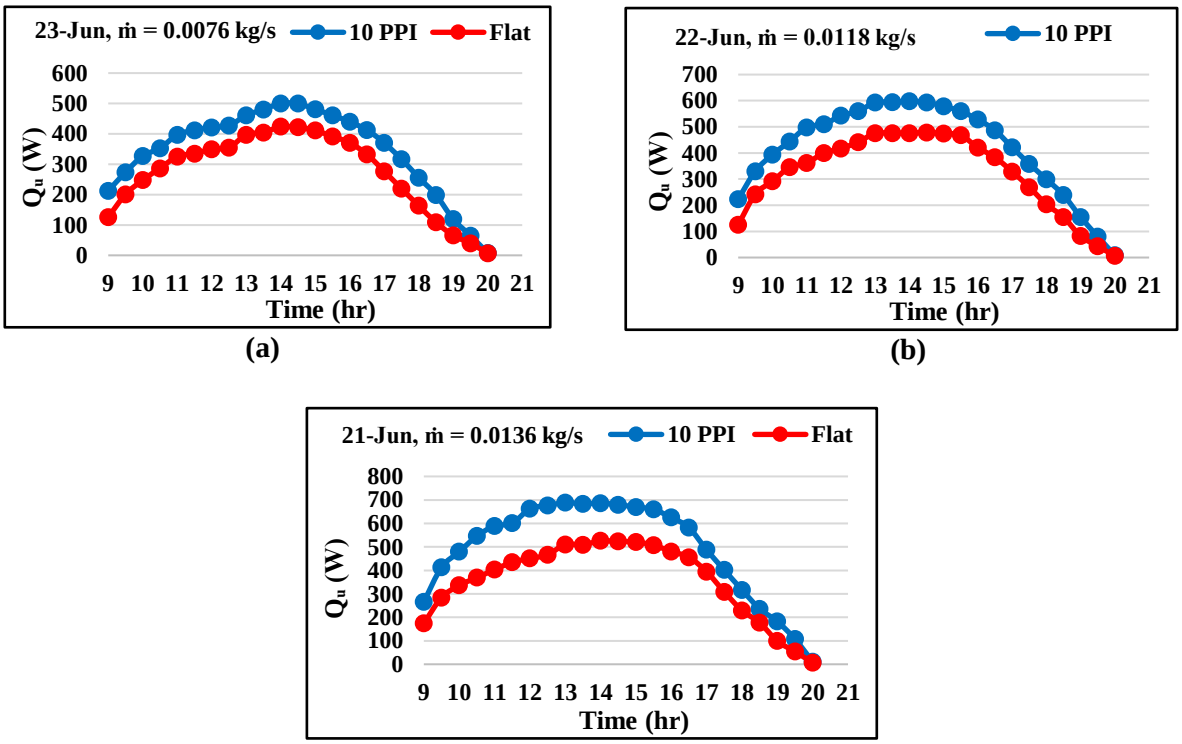

Fig. 6. Comparison between the heat transfer rate of DCSAH provided with flat and 10 PPI absorber plate

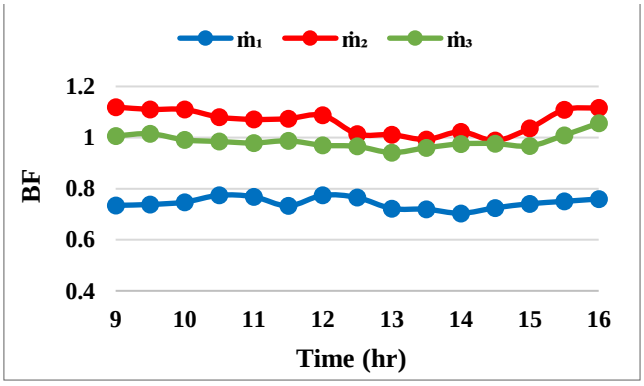

Fig. 7. Effect of **ṁ** on the benefit factor

Figure 8 and Fig. 9 present a time-dependent comparison of the thermal efficiency of a DCSAH featuring 10 PPI and flat absorber plates, both with and without the application of PCM. The results illustrate that the DCSAH's thermal performance, for both types of absorber plates (10 PPI and flat), without PCM, increases over time, directly influenced by incident solar radiation, reaching its peak value at 2:00 PM and gradually decreasing towards sunset. Furthermore, during the charging process, occurring between 9:00 AM and 3:00 PM, the DCSAHs' thermal performance without PCM exceeds that of those using PCM. However, post 3:00 PM during the discharging phase, solar collectors employing PCM exhibit greater thermal performance than those lacking PCM, attributed to the significant heat supplied by the PCM during the discharge process. Notably, after the period between 4:00 PM and 6:00 PM, the efficiency of the DCSAH equipped with PCM experiences a sharp increase, even surpassing 100% after sunset. Despite the enhanced DCSAH's thermal performance featuring a 10 PPI absorber plate, the air exit temperature from the collector remains excessively high. Considering the optimal temperature range for the desiccation of agricultural products lies within the bracket

of 45ºC and 60ºC [29], this elevated temperature renders it unsuitable for agricultural purposes. However, Fig. 10 illustrates the fluctuation of the DCSAH's air exit temperature with time for different ṁ on January 8th and 9th. Notably, the air exit temperature aligns well with the requirements for agricultural drying during these days. Consequently, the study concludes that the fabricated solar collector exhibits effective suitability for drying purposes, particularly during the winter season.

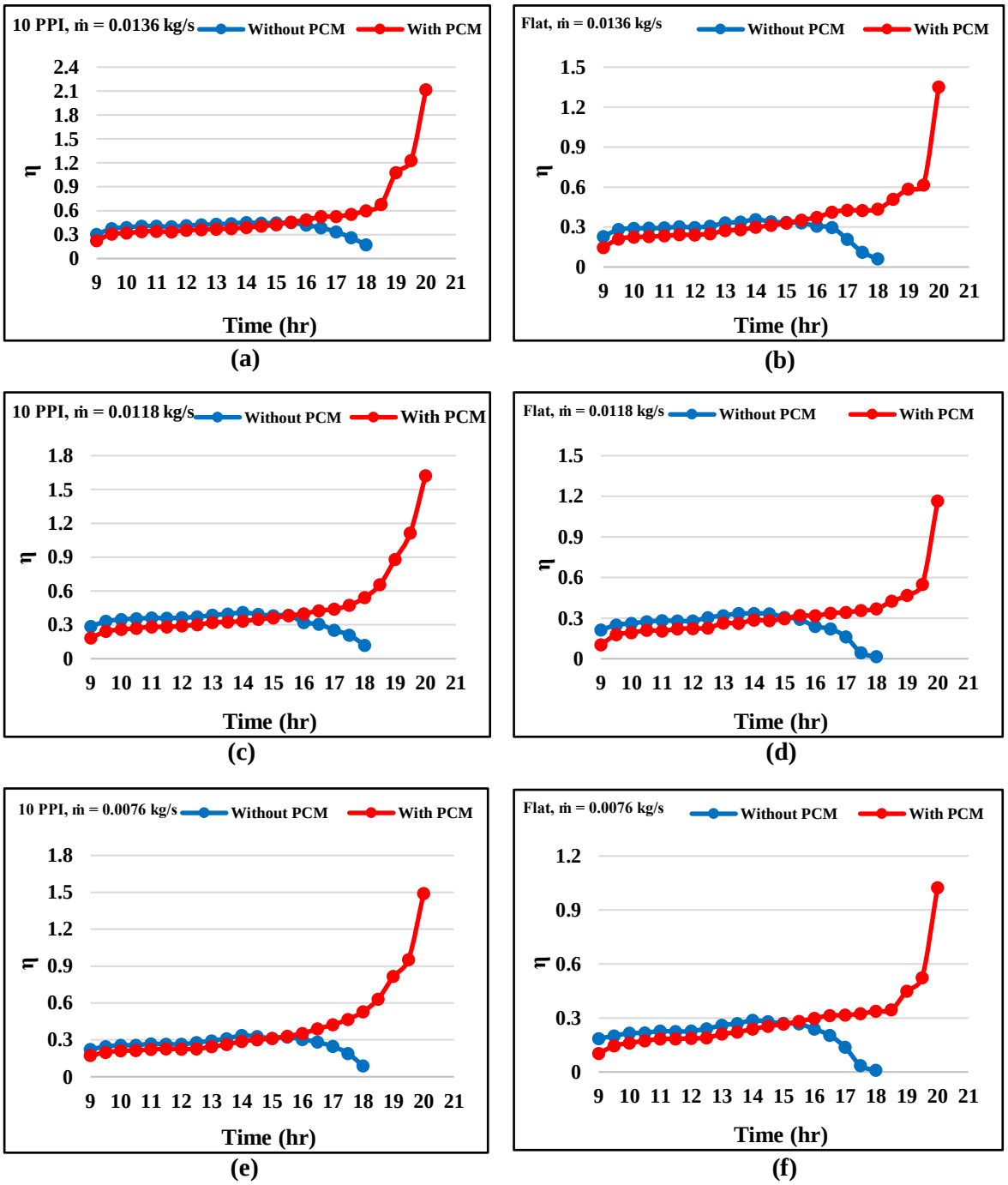

Fig. 8. PCM influence on the thermal efficiency of DCSAH featuring flat and 10 PPI absorber plates

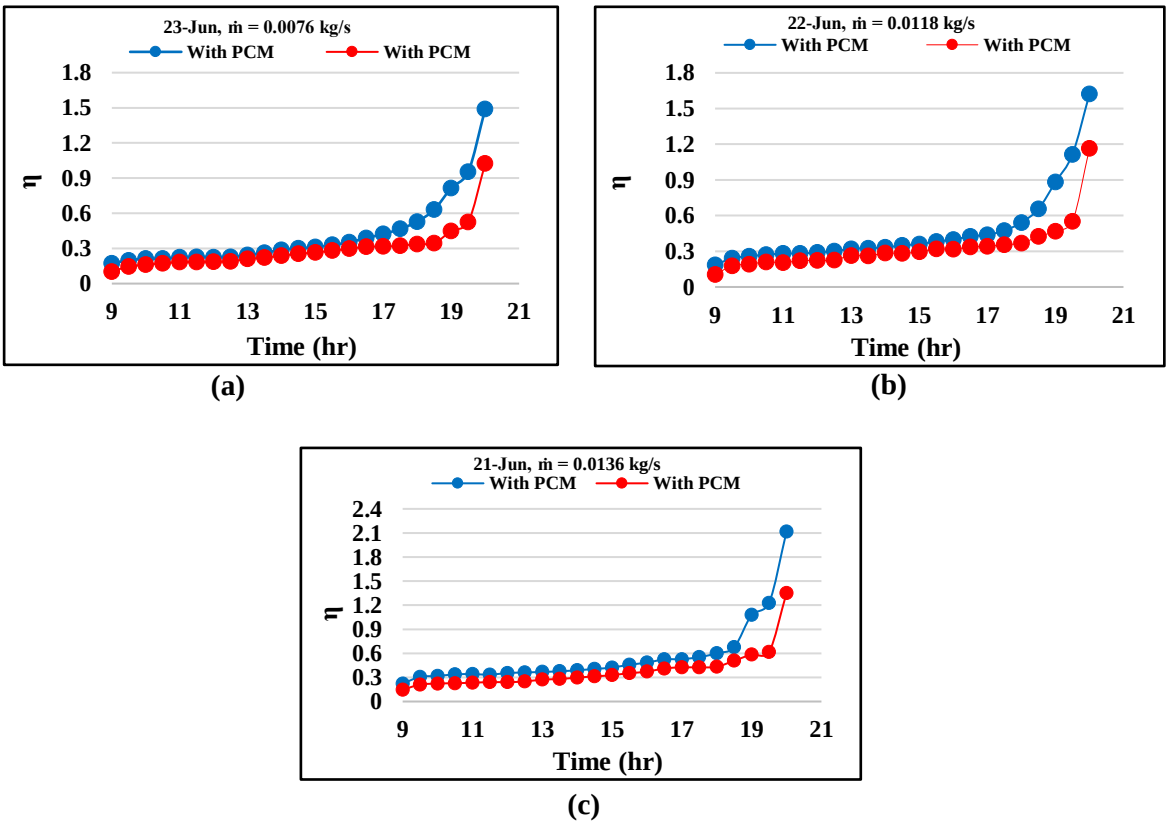

Fig. 9. A comparison between the DCSAH's thermal efficiency featuring flat and 10 PPI absorber plate

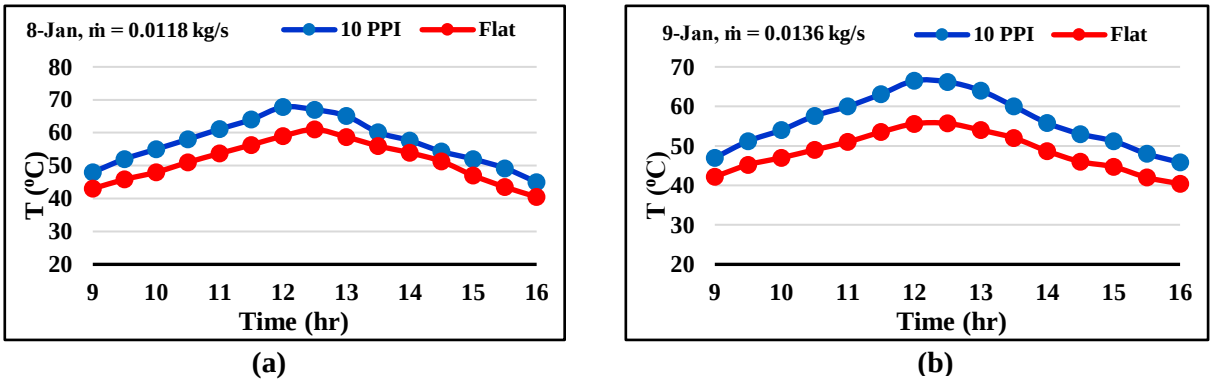

Fig. 10. Time-dependent air exit temperature of a DCSAH equipped with 10 PPI and flat absorber plates

Figure 11 presents a comparative examination of the DCSAH's heat transfer rate, with and without PCM, between the current study and a prior experimental study conducted by Mahmood [30] to validate the experimental results. The observed correlation in the behaviors between the present investigation and the earlier work indicates consistency in the findings. The heat transfer rate increases over time until reaching its peak, typically between 1:00 PM and 2:00 PM in the current investigation. Contrarily, in the previous work, the heat transfer rate peaked at 1:00 PM. This variation is attributed to differences in the design of the current system compared to that of the previous study. Further comparative analysis is implemented between the current experimental study and the previous research conducted by Krishnananth and Murugavel [31], as shown in Fig. 12. This comparison aims to evaluate the accuracy of the thermal efficiency behavior in the DCSAH, with and without PCM. The findings of the present study demonstrate a favorable concurrence with the findings of the earlier experimental work.

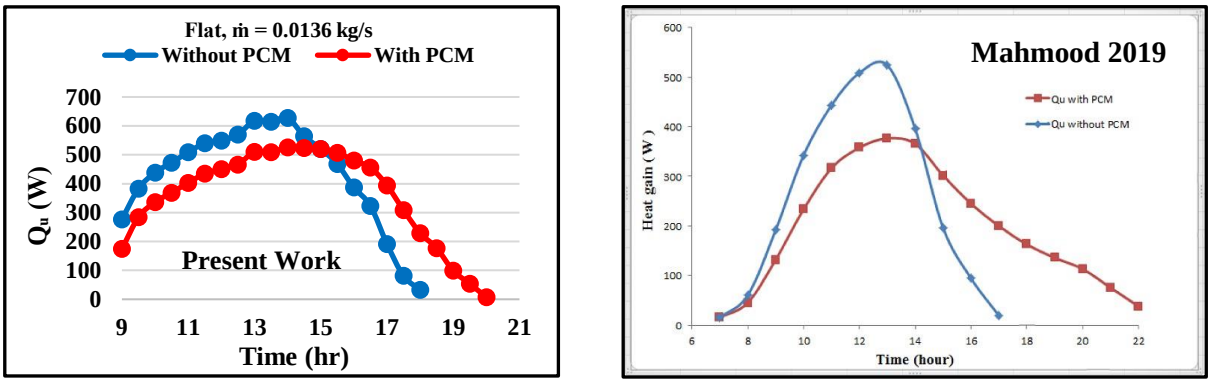

Fig. 11. Comparison of heat transfer rate between the present study and previous experimental work (Mahmood 2019)

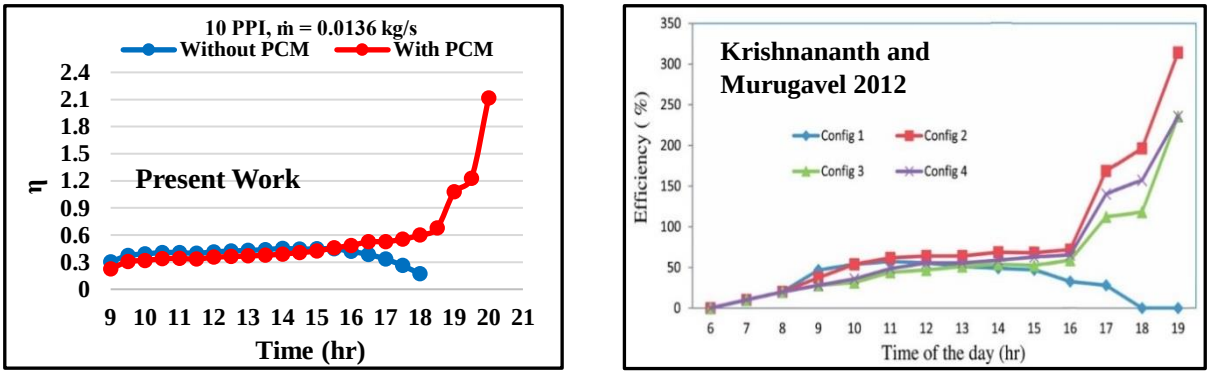

Fig. 12. Thermal efficiency comparison of the present study with previous experimental work (Krishnananth and Murugavel 2012)

5. Conclusion

the DCSAHs' thermal performance, both PCM-equipped and PCM-lacking, is analyzed, specifically focusing on incident solar radiation and rates of air mass flow. The results manifest that the DCSAH featuring a 10 PPI absorber demonstrates superior thermal performance in contrast to the flat absorber. Additionally, A rise in ṁ induces a reduction in temperature difference, resulting in higher heat transfer rates as well as improved thermal efficiency. The new solar collector exhibits a high Δi under conditions of elevated ṁ compared to a solar collector featuring a flat absorber. Consequently, to achieve a high thermal performance of the DCSAH with a copper foam absorber plate, it is advisable to supply a moderate ṁ. Furthermore, providing PCM results in elevations of the outlet air temperature over the ambient temperature by about 1 to 9 °C after sunset for two hours. The peak thermal efficiency of the 10 PPI absorber plate is recorded as 149%, 162%, and 211% for ṁ = 0.0076, 0.0118, and 0.0136 kg/s, correspondingly, while for a flat absorber plate, it is about 102%, 116%, and 135% for the same ṁ. The findings suggest that the DCSAH is applicable for drying purposes if the incident solar radiation is low or when more quantities of PCM are provided.

References

[1] Rabha DK, Muthukumar P. Performance studies on a forced convection solar dryer integrated with a paraffin wax–based latent heat storage system. Sol Energy. 2017;149:214-226.

[2] Jobair HK, Nima MA. The Indirect Solar Dryers with Innovative Solar Air Heaters. Designs: A Review Article. Heat Transfer.

[3] Mujumdar AS. Handbook of industrial drying. CRC Press; 2006.

[4] Karim MA, Hawlader MiN. Development of solar air collectors for drying applications.Energy Convers Manag. 2004;45(3):329-344.

[5] Abed QA, et al. Models for new corrugated and porous solar air collectors

under transient operation. J Non-Equilib Thermodyn. 2017;42(1):79-97.
[6] Aboghrara AM, et al. Performance analysis of solar air heater with jet impingement on corrugated absorber plate. Case Stud Therm Eng. 2017;10:111-120.
[7] Al-Juamily KEJ, Khalifa ABN, Yassen TA. Testing of the performance of a fruit and vegetable solar drying system in Iraq. Desalination. 2007;209(1-3):163-170.
[8] Vishnu N, et al. Modelling, dynamic simulation and parametric studies of double pass solar air heater for solar drying application. J Phys Conf Ser. 2021;2054(1).
[9] Al-Bakri BA, Rasham AR, AlSulttani AO. Thermal performance of multiple-pass solar air heater with pin fins. J Eng Sci Technol. 2022;17(3):2192-2217.
[10] Chabane F, Moummi N, Benramache S. Experimental study of heat transfer and thermal performance with longitudinal fins of solar air heater. J Adv Res. 2014;5(2):183-192.
[11] Peng D, et al. Performance study of a novel solar air collector. Appl Therm Eng. 2010;30(16):2594-2601.
[12] Hassan H, Yousef MS, Abo-Elfadl S. Energy, exergy, economic and environmental assessment of double pass V-corrugated-perforated finned solar air heater at different air mass ratios. Sustain Energy Technol Assess. 2021;43:100936.
[13] Taha SY, Farhan AA. Performance augmentation of a solar air heater using herringbone metal foam fins: An experimental work. Int J Energy Res. 2021;45(2):2321-2333.
[14] Abhay L, Chandramohan VP, Raju VRK. Numerical analysis on solar air collector provided with artificial square shaped roughness for indirect type solar dryer. J Clean Prod. 2018;190:353-367.
[15] Aldabbagh LBY, Egelioglu F, İlkan M. Single and double pass solar air heaters with wire mesh as packing bed. Energy. 2010;35(9):3783-3787.
[16] Omojaro AP, Aldabbagh LBY. Experimental performance of single and double pass solar air heater with fins and steel wire mesh as absorber. Appl Energy. 2010;87(12):3759-3765.
[17] Babar OA, et al. Design and performance evaluation of a passive flat plate collector solar dryer for agricultural products. J Food Process Eng. 2020;43(10):e13484.
[18] Ganesh A, Sudhakar P. Experimental investigation of phase change material based thermal storage system for solar dryer applications. Int J Pure Appl Math. 2017;117(7):331-343.
[19] Kalash AR, Shijer SS, Habeeb LJ. Thermal performance improvement of double pass solar air heater. J Mech Eng Res Dev. 2020;43(5):355-372.
[20] Aboul-Enein S, et al. Parametric study of a solar air heater with and without thermal storage for solar drying applications. Renew Energy. 2000;21(3-4):505-522.
[21] Enibe SO. Performance of a natural circulation solar air heating system with phase change material energy storage. Renew Energy. 2002;27(1):69-86.
[22] Sopian KB, Sohif M, Alghoul M. Output air temperature prediction in a solar air heater integrated with phase change material. Eur J Sci Res. 2009;27(3):334-341.
[23] Ramirez C, Palacio M, Carmona M. Reduced model and comparative analysis of the thermal performance of indirect solar dryer with and without PCM. Energies. 2020;13(20):5508.
[24] El Khadraoui A, et al. Thermal behavior of indirect solar dryer: Nocturnal usage of solar air collector with PCM. J Clean Prod. 2017;148:37-48.
[25] Alhusseny ANM, Nasser A, Al-zurfi NM. High-porosity metal foams: potentials, applications, and formulations. Porosity-Process, Technol Appl. 2018;181-200.
[26] Jobair HK, Abdullah OI, Atyia ZM. Feasibility study of a solar flat plate collector for domestic and commercial applications under Iraq climate. J Phys Conf Ser. 2018;1032(1).
[27] Gerhart PM, Gerhart AL, Hochstein JI. Munson, Young and Okiishi's Fundamentals of Fluid Mechanics. John Wiley & Sons; 2016.
[28] Webb RL, Kim NY. Enhanced heat transfer. Taylor & Francis; 2005.

[29] Agrawal A, Sarviya RM. A review of research and development work on solar dryers with heat storage. Int J Sustain Energy. 2016;35(6):583-605.

[30] Mahmood AS. Experimental study on double-pass solar air heater with and without using phase change material. J Eng. 2019;25(2):1-17.

[31] Krishnananth SS, Kalidasa Murugavel K. Experimental study on double pass solar air heater with thermal energy storage. J King Saud Univ Eng Sci.2013;25(2):135-140.